

Characterizing the stepwise transformation from a low-density to a very-high-density form of supercooled liquid water

Dietmar Paschek* and Alfons Geiger

Physikalische Chemie, Universität Dortmund, Otto-Hahn-Str. 6, D-44221 Dortmund, Germany

(Dated: September 1, 2017)

We explore the phase diagram of TIP4P-Ew [J. Chem. Phys. **120**, 9665 (2004)] liquid model water from the boiling-point down to 150 K at densities ranging from 0.950 g cm^{-3} to 1.355 g cm^{-3} . In addition to the low-density/high-density (LDL/HDL) liquid-liquid transition, we observe a high-density/very-high-density (HDL/VHDL) transformation for the lowest temperatures at 1.30 g cm^{-3} . A Van der-Waals type loop suggest the presence of a first order HDL/VHDL transition. In addition, we identify a pre-transition at 1.24 g cm^{-3} , suggesting the experimentally detected HDA/VHDA-transformation to be a two-step process. For both pre- and main- HDA/VHDA-transition we observe a step-wise increase of the oxygen coordination number for interstitial water molecules.

Experimental and theoretical studies conducted over the past 14 years have provoked the interpretation that water's anomalies stem from a transformation between two major liquid forms of water buried in the deeply supercooled region (see reviews by H.E. Stanley and P.G. Debenedetti [1, 2]). The two different liquids have their counterparts in the glassy state: The high density (HDA) and low density amorphous (LDA) ice forms [3]. However, it is still an open question how exactly the different amorphous ice forms and supercooled liquid water are connected, since the "no man's land" region largely prohibits direct experimental access [2]. Therefore, starting with the work of P.H. Poole et al. in 1992, basically computer simulation studies have established a picture of a first order liquid-liquid phase transition between two liquids ending up in a metastable critical point [4, 5]. Although singularity free scenarios might as well explain the properties of supercooled water [2], there is experimental support for the liquid-liquid critical point hypothesis from the changing slope of the metastable melting curves observed for different ice polymorphs [6, 7].

Meanwhile, also a very high density form (VHDA) of amorphous ice was observed and shown to be distinct from HDA [8]. Neutron scattering data reveals that the transformation between HDA and VHDA is related to an increasing population of interstitial water molecules in an O-O distance-interval between 3.1 \AA and 3.3 \AA [9]. Simulation studies indicate, that VHDA should be considered as the amorphous solid counterpart to the high density liquid water phase at ambient conditions, and not HDA [10, 11]. Koza et al. [12] have demonstrated by using inelastic neutron scattering that HDA and VHDA appear to be heterogeneous at the length-scale of nanometers and that different forms of HDA are obtained, depending on the exact preparation process [12]. Tulk et al. find by annealing of HDA at normal pressure [13] evidence for the presence of a multitude of (metastable) amorphous ice states. Finally, a very recent experimental study by Loerting et al. suggest the presence of a well established first order phase transition between the HDA and VHDA amorphous ices [14]. In this context we would like to em-

phasize, that the computer simulations of Brovchenko et al. [15, 16] were the first to conclude that there might exist even more than one liquid-liquid transition in supercooled water.

Here we present extensive thermophysical data on the deeply supercooled liquid state of the TIP4P-Ew water model [17]. TIP4P-Ew seems to be an ideal candidate, since it not only reproduces well the thermodynamic and structural properties of the liquid phase [17] (including a boiling point at 370 K [18]), but the TIP4P family of models also describe amazingly well the different ice polymorphs [19, 20, 21], qualitatively reproducing the entire phase diagram of crystal solid water up to about 1 GPa. Recently, also attempts have been undertaken to study the HDA to VHDA transition by computer simulations, suggesting a continuous structural transformation [22]. However, facing the low temperature conditions, these studies, although quite long on computer simulation time scales, suffer certainly from equilibration problems. To overcome these limitations, we present parallel tempering simulations of an extended ensemble of states [23], applying the technique of volume-temperature replica exchange molecular dynamics simulation (VTREMD) [24]. The Replica exchange molecular dynamics scheme (REMD), is a parallel tempering variant [25], based on the MD simulation technique, enhancing sampling by about two orders of magnitude [26].

For our simulation [27] we consider a grid of 644 (V, T) -states [28]. Starting from a set of equilibrated initial configurations obtained at ambient conditions, the simulation [29] was conducted for 50 ns, providing a total $32.2 \mu\text{s}$ worth of trajectory data. The average time interval between two successful state-exchanges was obtained to be about 3 ps. The overall shape of the phase diagram presented here is already well established after only 2 ns simulation time. However, since the configurational sampling of the lower- T states happens almost only by exchange with replicas coming from higher temperatures, the resolution of fine details of the PVT -diagram requires a long simulation run. The simulation took about 100 days on 20 Processors of our Intel Xeon 3.05 GHz Linux

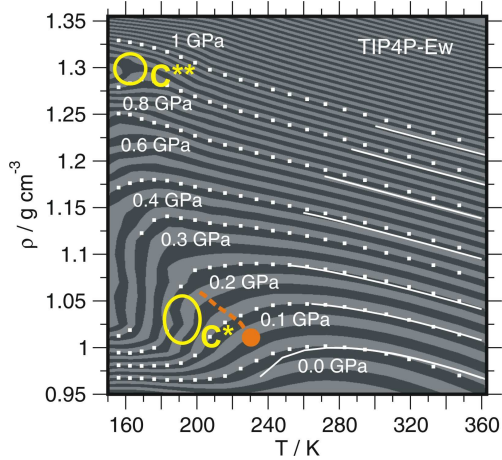


FIG. 1: $P(V,T)$ -surface of liquid TIP4P-Ew water [30]. The spacing between different contour colours corresponds to a pressure drop of 25 MPa. Selected isobars are indicated. The solid lines indicate the experimental isobars for 0.1 MPa, 0.1 GPa, 0.2 GPa, 0.4 GPa, 0.6 GPa, 0.8 GPa, and 1.0 GPa [31]. The ellipse indicates the as the LDL/HDL and HDL/VHDL critical regions for TIP4P-Ew. The large filled circle and the heavy dashed line indicates the metastable critical point and HDL/LDL-transition line for D₂O according to Mishima [7] projected on the TIP4P-EW $P(\rho, T)$ -surface.

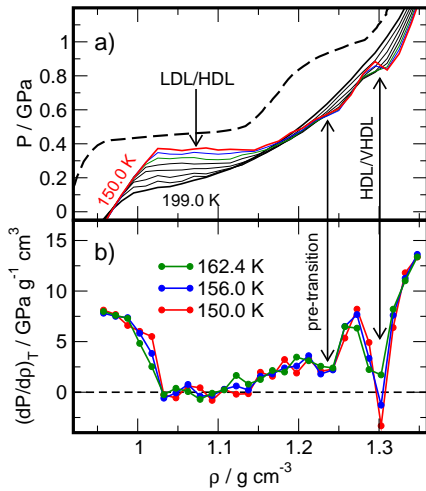


FIG. 2: a) Isotherms $P(\rho, T)$ for the eight lowest temperatures. The dashed line represents the compression curve of amorphous ice at 125 K according to Loerting et al. [14]. b) $\partial P(\rho, T)/\partial \rho_T$ for the three lowest temperature isotherms. The arrows indicate the location of the LDA/HDA and HDA/VHDA transitions, as well as the apparent pre-transition.

cluster. All data reported here were averaged over the final 45 ns of the simulation.

Figure 1 shows the phase diagram of liquid TIP4P-Ew water as contour plot of the $P(\rho, T)$ -data. The TIP4P-Ew phase diagram exhibits a first order low-density/high-density liquid-liquid phase transition, end-

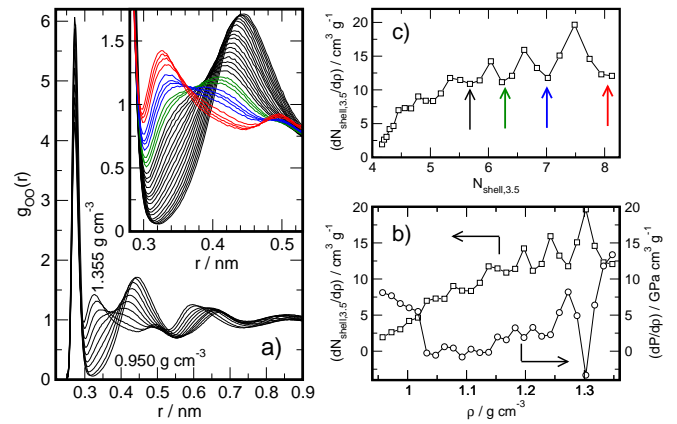


FIG. 3: a) OO radial pair distribution functions $g(r)$ for 150.0 K. Shown is every third density. The insert shows all OO- $g(r)$'s for the “interstitial region” for 150.0 K. Changing colour indicates gaps between the $g(r)$ -lines. b) Derivative of the pressure with respect to the density for the 150.0 K isotherm and derivative of the water coordination number ($r_{OO} \leq 0.35$ nm). respect to the density. c) Derivative of the water coordination number ($r_{OO} \leq 0.35$ nm). respect to the density as a function of the coordination number.

ing in a metastable critical point C^* . The ellipse denotes the region where LDL/HDL-critical point is apparently located. Due to a finer T -grid at lower temperatures, and longer simulation times, we have improved the sampling of the low- T states, compared to our recent study on the five-site TIP5P-E model [24]. Figure 1 demonstrates that TIP4P-Ew reproduces the experimental phase diagram of liquid water much better than the TIP5P-E model [24], almost quantitatively matching waters compressibility and thermal expansivity up to pressures in the GPa-range. Figure 1a indicates, that the Van der Waals-loop like overshooting of the $P(\rho, T)$ -isotherm, as observed in the HDL/LDL coexistence region of the TIP5P-E model [24], is found to be almost completely flattened out in the case of TIP4P-Ew. Also shown in Figure 1 is the LDL/HDL-transition line and critical point as obtained by O. Mishima [7] for D₂O. Since the densities of the experimental coexistence line are essentially not known, we have projected the pressures reported by Mishima on the TIP4P-Ew $P(\rho, T)$ -surface. We find a temperature difference between the two metastable critical points by about 30 – 40 K. We would like to point out that this value corresponds roughly to the temperature difference between the Ice- I_h melting-lines of TIP4P-Ew and D₂O [20].

In addition to the LDL/HDL-transition, we denote the appearance of another (HDL/VHDL) liquid-liquid-transition at 1.30 g cm^{-3} at about 165 K. The second metastable critical region, denoted by C^{**} , is identified by a van der Waals type of behavior of P vs. ρ shown in Figure 2a. Moreover, Figure 2b presents the derivative $(\partial P(\rho, T)/\partial \rho)_T$ of the lower- T isotherms character-

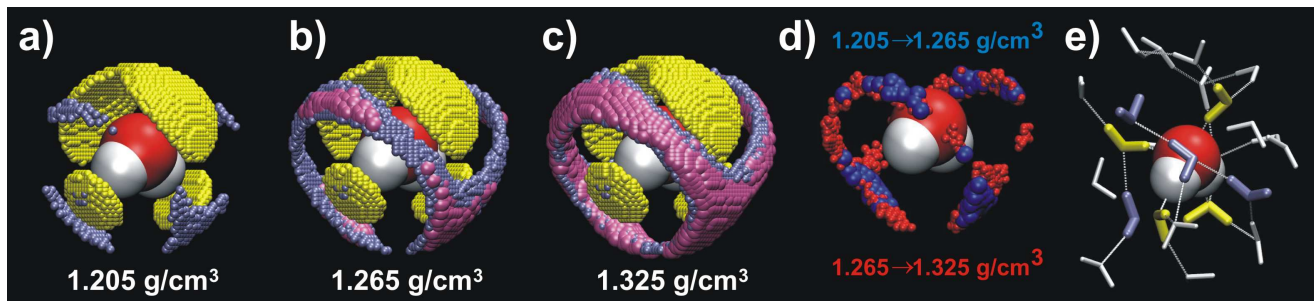


FIG. 4: a,b,c) 3D-distribution of water density around a central water molecule. Each small sphere represents a volume element with a water number density larger than 100 nm^{-3} whereas the larger (mauve) spheres indicate densities exceeding then 130 nm^{-3} . Yellow indicates the first shell ($r \leq 0.3 \text{ nm}$), whereas iceblue and mauve indicate interstitial water ($r < 0.3 \leq 0.35 \text{ nm}$). Densities are indicated, $T = 150 \text{ K}$. d) Volume elements showing a numer density increase of more than 45 nm^{-3} when increasing the density $1.205 \text{ g cm}^{-3} \rightarrow 1.265 \text{ g cm}^{-3}$ (blue) and $1.265 \text{ g cm}^{-3} \rightarrow 1.325 \text{ g cm}^{-3}$ (red) at 150.0 K . e) Snapshot of a randomly selected solvation shell of a water molecule, 1.325 g cm^{-3} at 150.0 K . Color coding is as in a.

izing the HDL/VHDL-transition by a pronounced dip. In addition to the fully developed first order transition at 1.30 g cm^{-3} , we would like to point out the appearance of a shoulder at about 1.24 g cm^{-3} (Figure 2a), corresponding to a less well pronounced dip in Figure 2b. Both curves indicate the emergence of a not yet fully developed transition around 1.24 g cm^{-3} , which we refer to as the HDL/VHDL *pre-transition*. We find that our simulations are in qualitative agreement with the experimental compression curve of amorphous water obtained at 125 K shown in Figure 2a. However, there is a shift of about 0.06 g cm^{-3} between the experimental and simulated data-sets. The elastic compression of VHDA as obtained by Loerting et al. with $0.10 \text{ g cm}^{-3} \text{ GPa}^{-1}$ [14] is comparable to the $0.08 \text{ g cm}^{-3} \text{ GPa}^{-1}$ (Figure 2b) of the VDHL-phase observed here. The *larger* elastic compression found for HDA ($\approx 0.14 \text{ g cm}^{-3} \text{ GPa}^{-1}$ [14]) is also qualitatively in accordance with our simulation data. Moreover, the slightly asymmetric shape of HDA/VHDA the transition observed by Loerting et al. [14] over the density interval between 1.18 g cm^{-3} 1.30 g cm^{-3} does not seem to rule out the presence of a softer transition or pre-transition in the density range of 1.22 g cm^{-3} to 1.24 g cm^{-3} and a sharper transition at about 1.28 g cm^{-3} .

Figure 3 shows how the observed transitions are related to structural changes in the local environment of the water molecules. Figure 3a depicts the O-O pair correlation functions for water at 150 K as a function of density. The insert given in Figure 3a focuses primarily on the changes in the so called interstitial water region between 0.3 nm and 0.35 nm . In line with structural data obtained from neutron scattering experiments [9], we observe the appearance of a peak in the interstitial region as pressure increases. Moreover, with increasing density we denote the occurrence *undulations* in the water coordination number. In the insert in Figure 3a these undulations appear as larger gaps between the individual $g(r)$ -curves.

For better visibility these increased gaps are indicated by a changing color. The magnitude of the variation in the local density is shown in Figure 3b by plotting derivative of waters O-O coordination number for $r \leq 0.35 \text{ nm}$ with respect to the density $(\partial N_{3.5}/\partial \rho)_T$. Comparing this data with the $(\partial P(\rho, T)/\partial \rho)_T$ -line (Figure 3b) we find that the observed HDL/VHDL transitions are exactly accompanied by a step-wise increase of water’s coordination number. Moreover, Figure 3b presents the $(\partial N_{3.5}/\partial \rho)_T$ data as a function of the coordination number $N_{3.5}$. The diagram indicates that the HDL/VHDL transition is accompanied by an increase from seven to eight water molecules in the sphere of 0.35 nm around a central water molecule. At the HDL/VHDL pre-transition we find only a fractional increase of about 0.75 water molecules on average. Further wiggles in $(\partial N_{3.5}/\partial \rho)_T$ suggest that there is at least one more step in the occupation number at even lower densities.

Figure 4 illustrates the structural changes of the local water environment along the HDL/VHDL pre- and main-transitions. In line with experimental finding, waters first coordination shell ($r \leq 0.3 \text{ nm}$) is found to consist of four tetrahedrally arranged water molecules [9]. With increasing pressure, water is penetrating the interstitial region ($0.3 \text{ nm} \leq r \leq 0.35 \text{ nm}$) arranging in a lobes around the positions occupied by the first-shell water molecules. However, even at the highest densities there are not more than about four water molecules filling the interstitial positions, indicating that the lobe-type positions can be only partially occupied. Figure 4a indicates that for HDL-water the interstitial molecules are preferentially located on the “anti-tetrahedral” positions, being located on the centers of faces of the tetrahedron formed by the first-shell water molecules. Figure 4b and 4d indicate that along the pre-transition interstitial water is also predominantly inserting into these “anti-tetrahedral” positions, whereas during the HDL/VHDL main-transition the lobes are getting more and more

completed by increasingly filling the gaps between two “anti-tetrahedral” sites. Figure 4e exemplifies this scenario, showing four nearest neighbor water molecules and three water molecules in “anti-tetrahedral”-coordination. The water molecule representing on the connecting lobe-position is apparently forming a hydrogen bond-bridge between the water molecules.

In conclusion, our simulations indicate the presence of a major HDL/LDL transition in supercooled water, being responsible for the anomalous thermodynamical behavior of water at ambient conditions. However with decreasing temperature, water’s $P(\rho, T)$ surface becomes increasingly corrugated, developing further step-like transformations: The HDL/VHDL pre- and main-transitions, and possibly more at even lower temperatures. The onset of these transformations is apparently tightly related to a change of the local coordination of the water molecules. Hence we propose a two-region scenario for supercooled-water: A very low-temperature region with several distinct structural transitions, which is typically probed by studies on the amorphous forms of water [8, 12, 13, 14], and a medium temperature region, where due to increased thermal energy these transitions are covered and two major liquid forms of water (LDL and HDL) are found to be in equilibrium.

We gratefully acknowledge support by the Deutsche Forschungsgemeinschaft (FOR 436).

* Electronic address: dietmar.paschek@udo.edu

- [1] P. G. Debenedetti and H. E. Stanley, *Physics Today* **56**, 40 (2003).
- [2] P. G. Debenedetti, *J. Phys. Cond. Matt.* **15**, R1669 (2003).
- [3] O. Mishima, L. D. Calvert, and E. Whalley, *Nature* **310**, 393 (1984).
- [4] P. H. Poole, F. Sciortino, U. Essmann, and H. E. Stanley, *Nature* **360**, 324 (1992).
- [5] H. Tanaka, *Nature* **380**, 328 (1996).
- [6] O. Mishima and H. E. Stanley, *Nature* **396**, 329 (1998).
- [7] O. Mishima, *Phys. Rev. Lett.* **85**, 334 (2000).
- [8] T. Loerting, C. Salzmann, I. Kohl, E. Mayer, and A. Hallbrucker, *Phys. Chem. Chem. Phys.* **3**, 5355 (2001).
- [9] J. L. Finney, D. T. Bowron, A. K. Soper, T. Loerting, E. Mayer, and A. Hallbrucker, *Phys. Rev. Lett.* **89**, 205503 (2002).
- [10] N. Giovambattista, H. E. Stanley, and F. Sciortino, *Phys. Rev. Lett.* **94**, 107803 (2005).
- [11] N. Giovambattista, H. E. Stanley, and F. Sciortino, *Phys. Rev. E* **72**, 031510 (2005).
- [12] M. M. Koza, B. Geil, K. Winkel, C. Köhler, F. Czeschka, M. Scheuermann, H. Schober, and T. Hansen, *Phys. Rev. Lett.* **94**, 125506 (2005).
- [13] C. A. Tulk, C. J. Benmore, J. Urquidi, D. D. Klug, J. Neufeind, B. Tomberli, and P. A. Egelstaff, *Science* **297**, 1320 (2002).
- [14] T. Loerting, W. Schustereder, K. Winkel, C. Salzmann, I. Kohl, and E. Meyer, *Phys. Rev. Lett.* (2005), (in print).
- [15] I. Brovchenko, A. Geiger, and A. Oleinikova, *J. Chem. Phys.* **118**, 9473 (2003).
- [16] I. Brovchenko, A. Geiger, and A. Oleinikova, *J. Chem. Phys.* **123**, 044515 (2005).
- [17] H. W. Horn, W. C. Sope, J. W. Pitera, J. D. Madura, T. J. Dick, G. L. Hura, and T. Head-Gordon, *J. Chem. Phys.* **120**, 9665 (2004).
- [18] H. W. Horn, W. C. Swope, and J. W. Pitera, *J. Chem. Phys.* **123**, 194504 (2005).
- [19] E. Sanz, C. Vega, and J. L. F. Abascal, *Phys. Rev. Lett.* **92**, 255701 (2004).
- [20] C. Vega, E. Sanz, and J. L. F. Abascal, *J. Chem. Phys.* **122**, 114507 (2005).
- [21] C. Vega, J. L. F. Abascal, E. Sanz, L. G. MacDowell, and C. McBride, *J. Phys.: Condens. Matter* **17**, S3283 (2005).
- [22] R. Martoňák, D. Donadio, and M. Parrinello, *J. Chem. Phys.* **122**, 134501 (2005).
- [23] E. Marinari and G. Parisi, *Europhys. Lett.* **19**, 451 (1992).
- [24] D. Paschek, *Phys. Rev. Lett.* **94**, 217802 (2005).
- [25] Y. Sugita and Y. Okamoto, *Chem. Phys. Lett.* **314**, 141 (1999).
- [26] R. Yamamoto and W. Kob, *Phys. Rev. E* **61**, 5473 (2000).
- [27] State swapping moves between two states i and j are accepted with a probability $P_{acc} \min\{1, \exp[\beta_i (U(\vec{s}_i^N; L_i) - U(\vec{s}_j^N; L_i))] + \beta_j (U(\vec{s}_j^N; L_j) - U(\vec{s}_i^N; L_j))\}$. Here, \vec{s}_i^N represents the set of scaled coordinates $\vec{s}_N = L^{-1} \vec{r}_N$ of the entire N -particle system belonging to state i . $U(\vec{s}_i^N; L_i)$ denotes the potential energy of configuration \vec{s}_i^N at volume $V_i = L_i^3$, whereas $U(\vec{s}_i^N; L_j)$ represents the configurational energy belonging to \vec{s}_i^N at volume V_j . Whether a state swapping move or an MD move is executed, is chosen at random with a probability of 0.2 for selecting state swapping moves.
- [28] Temperatures 150.0 K, 156.0 K, 162.4 K, 169.0 K, 176.0 K, 183.3 K, 191.0 K, 199.0 K, 207.3 K, 215.8 K, 224.6 K, 233.5 K, 242.7 K, 252.1 K, 261.9 K, 272.2 K, 283.0 K, 294.4 K, 306.4 K, 319.2 K, 332.9 K, 347.4 K, 362.8 K at densities between 0.950 g cm^{-3} and 1.355 g cm^{-3} with an increment of 0.015 g cm^{-3} .
- [29] Each replica represents a MD simulation of 256 molecules in the NVT ensemble. The electrostatic interactions are treated by Ewald summation [32] with a cutoff of 0.9 nm and a $18 \times 18 \times 18$ mesh with 4th order interpolation. Lennard-Jones cutoff corrections for energy and pressure were considered. A 2 fs timestep was used. The simulations were carried out with GROMACS 3.2 (www.gromacs.org), modified by us to allow V, T -state-swapping. The temperature tiling has been chosen to maintain an acceptance ratio of about 0.2 for state swapping.
- [30] The PVT -data is available from, URL <http://ganter.chemie.uni-dortmund.de/TIP4PEw.html>.
- [31] W. Wagner and A. Pruß, *J. Phys. Chem. Ref. Data* **31**, 387 (2002).
- [32] U. Essmann, L. Perera, M. L. Berkowitz, T. A. Darden, H. Lee, and L. G. Pedersen, *J. Chem. Phys.* **103**, 8577 (1995).